*Journal of Biomolecular NMR*, **25:** 147–152, 2003.
*KLUWER/ESCOM*



# A new strategy for backbone resonance assignment in large proteins using a MQ-HACACO experiment

Konstantin Pervushin* & Alexander Eletsky
*Laboratorium für Physikalische Chemie, Eidgenössische Technische Hochschule Hönggerberg, CH-8093 Zurich, Switzerland*

Received 15 July 2002; Accepted 25 October 2002

*Key word:* backbone resonance assignment

## Abstract

A new strategy of backbone resonance assignment is proposed based on a combination of the most sensitive TROSY-type triple resonance experiments such as TROSY-HNCA and TROSY-HNCO with a new 3D multiple-quantum HACACO experiment. The favourable relaxation properties of the multiple-quantum coherences and signal detection using the $^{13}C'$ antiphase coherences optimize the performance of the proposed experiment for application to larger proteins. In addition to the $^{1}H^{N}$, $^{15}N$,$^{13}C^{\alpha}$ and $^{13}C'$ chemical shifts the 3D multiple-quantum HACACO experiment provides assignment for the $^{1}H^{\alpha}$ resonances in constrast to previously proposed experiments for large proteins. The strategy is demonstrated with the 44 kDa uniformly $^{15}N$,$^{13}C$-labeled and fractionally 35% deuterated trimeric *B. subtilis* Chorismate Mutase measured at 20 °C and 9 °C. Measurements at the lower temperature indicate that the new strategy can be applied to even larger proteins with molecular weights up to 80 kDa.

*Abbreviations:* TROSY, transverse relaxation-optimized spectroscopy; MQ, multiple quantum; nD, *n*-dimensional.

## Introduction

Transverse relaxation-optimized spectroscopy (TROSY) (Pervushin et al., 1997) yields substantial reduction of the transverse relaxation rates in $^{15}N$-$^{1}H^{N}$ moieties by constructive use of the interference between DD coupling and chemical shift anisotropy (CSA) interactions. Previously, the implementation of [$^{15}N$,$^{1}H$]-TROSY in the HNCA and HNCO experiments (Salzmann et al., 2000) yielded several-fold sensitivity improvement when applied to larger $^{2}H$/$^{13}C$/$^{15}N$-labeled proteins, and a significant gain in sensitivity was also obtained for protonated proteins. In recent years 3D and 4D TROSY versions of the conventional triple-resonance experiments have been developed (Salzmann et al., 1999a, b; Yang and Kay, 1999; Mulder et al., 2000). Although these experiments have proven robust in the process of sequential assignment of the backbone resonances in large proteins (Pervushin, 2000), there are inherent problems associated with the $^{1}H^{N}$ 'out-and-back' method underlying this line of experiments. These are: (i) In TROSY-HNCA and HN(CA)CO-type experiments sequential cross-peaks are usually observed with lower sensitivity than their intraresidual counterparts due to the smaller values of the scalar couplings $^{2}J_{NC\alpha}$ relative to $^{1}J_{NC\alpha}$ (Cavanagh et al., 1996); (ii) the use of TROSY-HN(CO)CA-type experiments is limited to spectrometers operating at lower polarizing magnetic field strength, $B_0$, due to the quadratic dependence of the $^{13}C'$ transverse relaxation rates on $B_0$ (Dayie and Wagner, 1997) and the necessity to employ transverse $^{13}C'$ coherences evolving during two constant time 'out-and-back' magnetization transfer periods (Salzmann et al., 1999b); (iii) the assignment process is interrupted at prolyl residues.

Here we propose a new 3D multiple-quantum HACACO experiment with direct detection of the $^{13}C'$

*To whom correspondence should be addressed. E-mail: kopeko@phys.chem.ethz.ch

antiphase coherence to alleviate the first two of the problems mentioned above. The experiment relies on the favorable relaxation properties of the multiple quantum coherences (Grzesiek et al., 1995; Swapna et al., 1997; Xia et al., 2000) to record $^1H^\alpha$ and $^{13}C^\alpha$ chemical shifts and transfer the $^1H^\alpha$ magnetization to the $^{13}C'$ spins using one double- constant-time evolution period (Swapna et al., 1997). High sensitivity and a simple doublet structure of the $^{13}C'$ resonances enable the effective signal acquisition even for large proteins. Our experiment differs from previous implementations of the $^1H^\alpha$-start and $^{13}C'$-observe approach (Serber et al., 2000, 2001) by the use of (i) multiple quantum sensitivity improvement, (ii) a single constant time polarization transfer period, (iii) signal detection via the $^{13}C'$ antiphase doublet and (iv) optimized $^1H^\alpha$ recovery to thermal equilibrium achieved by returning the $^1H^N$ magnetization to the +z direction before signal acquisition. The MQ-HACACO experiment suggests a new strategy for backbone resonance assignment in larger proteins by bridging the 3D TROSY-HNCA and TROSY-HNCO experiments. The strategy is demonstrated here by measurements with a 44 kDa trimeric $^{13}C$- and $^{15}N$-labeled protein at 20 °C and 9 °C.

Figure 1 depicts the pulse sequence of the 3D MQ-HACACO experiment based on the HMQC double-constant-time magnetization transfer scheme and direct detection of the $^{13}C'$ coherence antiphase relative to the $^{13}C^\alpha$ spins. In short, product operator descriptions of the coherence transfer pathways is $H_z^\alpha \rightarrow H_y^\alpha(t_1) \rightarrow -2H_x^\alpha C_z^\alpha(t_1) \rightarrow 2H_x^\alpha C_y^\alpha(t_1,t_2) \rightarrow -4H_x^\alpha C_x^\alpha C_z'(t_1,t_2) \rightarrow H_z^\alpha C_x^\alpha C_z'(t_2) \rightarrow C_y^\alpha C_z'(t_2) \rightarrow 2C_z^\alpha C_y'(t_3)$, where $H^\alpha$, $C^\alpha$ and $C'$ are the angular momentum operators of $^1H^\alpha$, $^{13}C^\alpha$ and $^{13}C'$ spins, respectively. Two $^1H^N$ band-selective 90° pulses are introduced to return the $^1H$ spins resonating between 7.4 ppm and 10 ppm to the +z direction before signal acquisition, which shortens the optimal interscan delay by 20% (see below). The experimental scheme of Figure 1 is best suited for the methine $C^\alpha$ carbons since the full use of the double-constant-time period can be made for the $^1H^\alpha$ and $^{13}C^\alpha$ chemical shift evolution. A modification of the experimental scheme of Figure 1 is required in order to detect the methylene $C^\alpha$ carbons as occurs in glycine residues with optimal sensitivity. This version of the HACACO corresponds to the first part of the (HA)CA(CO)NH experiment introduced by (Swapna et al., 1997) and will not be described in detail in this communication.

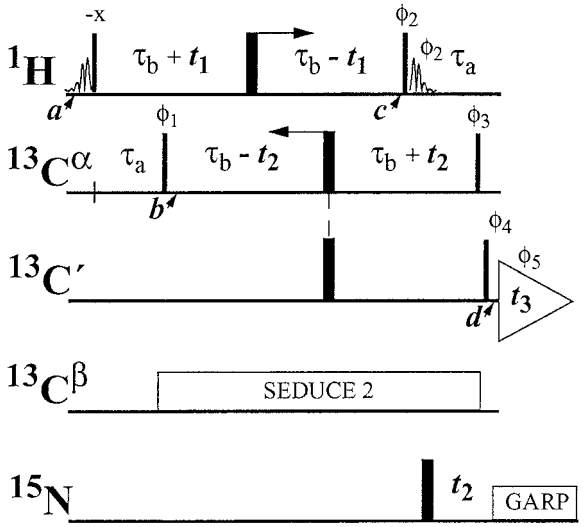


*Figure 1.* Experimental scheme for the 3D MQ-HACACO experiment. The radio-frequency pulses on $^1H$, $^{15}N$, $^{13}C^\alpha$, $^{13}C^\beta$ and $^{13}C'$ are applied at 4.7, 118, 55, 22.5 and 174 ppm, respectively. Narrow and wide black bars indicate non-selective 90° and 180° pulses, respectively. Shaped pulses on the line marked $^1H$ are the $^1H^N$ band-selective 2.2 ms excitation E-Burp2 pulse (Geen and Freeman, 1991) with $\gamma B_1 = 1900$ Hz and the time-reversed excitation E-Burp2 pulse with the phase $\phi_2$. The center of excitation for the $^1H^N$ band-selective pulses is placed at 8.7 ppm, so that all amide protons resonating between 10 and 7.4 ppm are returned to the +z axis. The time delays $\tau_a = 1(2\,^1J_{HC})$ and $\tau_b = 1(4\,^1J_{C^\alpha C'})$ are set to 3.2 ms and 4.5 ms, respectively. The phases are: $\phi_1 = \{x, -x\}$; $\phi_2 = \{2x, 2(-x)\}$; $\phi_3 = \{4x, 4(-x)\}$; $\phi_4 = \{8x, 8(-x)\}$; $\phi_5 = \{x, -x, -x, x, -x, x, x, -x, -x, x, x, -x, x, -x, -x, x\}$; and $\{x\}$ for all other pulses. Quadrature detection in the $^1H^\alpha(t_1)$ and $^{13}C^\alpha$ ($t_2$) dimensions is achieved by the States-TPPI method (Marion et al., 1989) applied to the phases $\phi_2$ and $\phi_3$, respectively. The 3D spectrum is processed as described (see text and Figure 3) in order to remove the antiphase splitting of the $^{13}C'$ resonances. At the polarizing magnetic field strength of 600 MHz the durations of the rectangular $^{13}C^\alpha$ and $^{13}C'$ 90° and 180° pulses are 48 and 47 μs, respectively. The $^{13}C^\alpha$ and $^{13}C'$ 180° pulses are performed simultaneously to minimize effects due to off-resonance excitation of $^{13}C^\alpha$ spins induced by the $^{13}C'$ pulse. Selective $^{13}C^\beta$ decoupling is achieved by SEDUCE2 (Shaka et al., 1983) at a field strength of $\gamma B_2 = 560$ Hz.

A good quality 3D MQ-HACACO spectrum is obtained for the 44 kDa uniformly $^{15}N$,$^{13}C$-labeled and fractionally 35% deuterated chorismate mutase from *Bacillus subtilis* (BsCM) (Eletsky et al., 2001) using the experimental scheme of Figure 1. Figure 2a shows a [$^{13}C'$,$^1H^\alpha$] projection of the Fourier transformed 3D data set. The key element of the new experiment is the post-acquisition superposition of the negative and positive components of the $2C_z^\alpha C_y'$ antiphase doublet. Figure 2b shows the same projection of the 3D MQ-HACACO spectrum obtained with the procedure described in Figure 3 where only single cross-peak

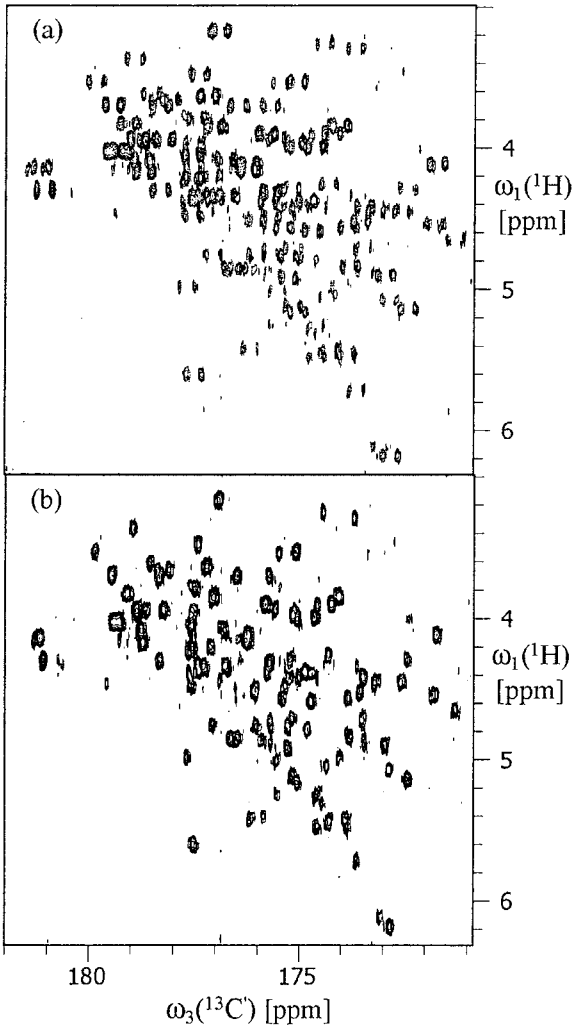


*Figure 2.* $^{1}H^{\alpha}$-$^{13}C'$ Projection from a 3D MQ-HACACO experiment recorded with the 44 kDa uniformly $^{15}N$,$^{13}C$-labeled and fractionally 35% deuterated BsCM (Eletsky et al., 2001) in $^{1}H_2O$:$^{2}H_2O$ (97:3) solution (protein concentration 1 mM, pH = 7.5, 20 °C) on a Bruker Avance 600 spectrometer equipped with a $^{1}H$-, $^{2}H$-, $^{13}C$- and $^{15}N$-tunable and $^{1}H$-observe CryoProbe using the experimental scheme of Figure 1. $20(t_1)\times36(t_2)\times512(t_3)$ complex points were accumulated yielding $t_{1\,max}$ = 9 ms, $t_{2\,max}$ = 9 ms and $t_{3\,max}$ = 200 ms, respectively. An interscan delay of 800 ms and 24 scans per increment were used resulting in a total measuring time of 20 h. The projections in (a) and (b) are taken from the 3D spectra processed without and with the post-acquisition superposition of negative and positive components of the antiphase doublets (see text and Figure 3), respectively.

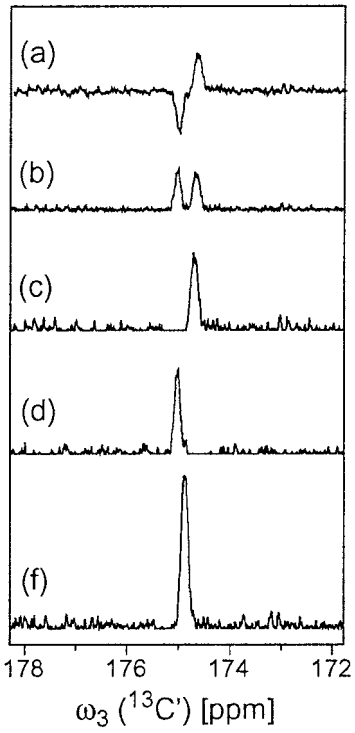


*Figure 3.* Sensitivity enhancement by post-acquisition superposition of negative and positive components of the 3D antiphase doublets. 1D slices along the $\omega_3(^{13}C')$ dimension are taken through the positions of the cross-peak of Ile53 in the 3D MQ-HACACO spectrum of the figure at various stages of post-acquisition processing. (a) The starting spectrum. (b) The absolute value of (a). (c) and (d) Two linear combinations of (a) and (b) resulting in the recovery of the 'left' and 'right' $^{13}C'$ multiplet components. (f) The final spectrum obtained by addition of the spectra (c) and (d) after shifting them by +26.5 Hz and −26.5 Hz, respectively. The S/N in (f) is increased by $\sqrt{2}$ relative to (a). Identical vertical scaling is applied to all 1D slices.

per residue is obtained. The post-acquisition processing of the spectra relies on pure antiphase character of the doublet. That, in turn, is ensured by the fact that the $^{1}J_{C^{\alpha}C'}$ coupling constants show only minor variation throughout the polypeptide backbone. A sensitivity enhancement of factor was observed for all resolved backbone signals (Figure 3f) after linear recombination of the original spectrum (Figure 3a) with the absolute value representation of the same spectrum (Figure 3b). Individual doublet components of the $^{13}C'$ resonances can be reconstructed even for the heavily overlapping signals. In this case, however, smaller gains in sensitivity are obtained. In contrast to advanced nonlinear signal reconstruction methods (Koehl, 1999; Serber et al., 2000) this simple and ro-

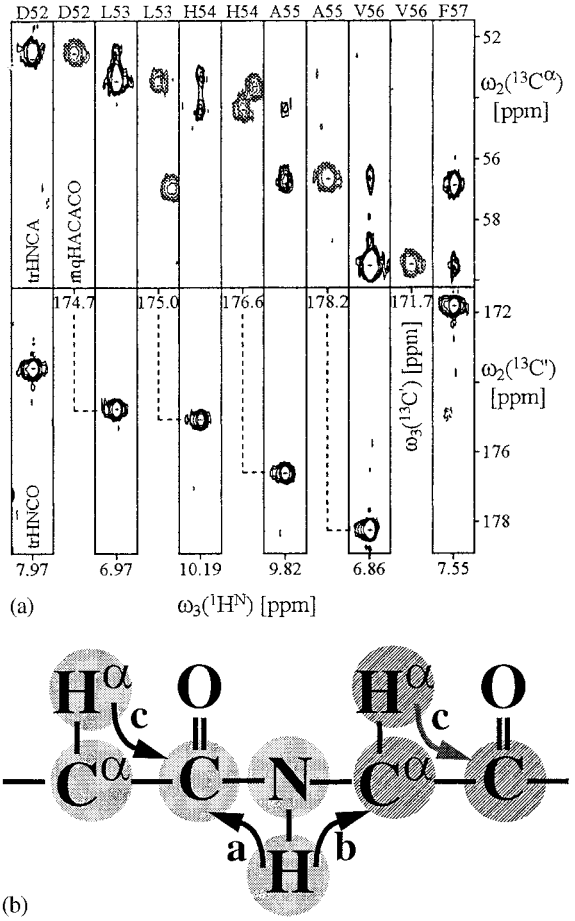


*Figure 4.* Strategy of assignment of the backbone $^{1}H^{\alpha}$, $^{13}C'$, $^{13}C^{\alpha}$ and $^{15}N$ resonance in uniformly $^{13}C$, $^{15}N$-labeled and fractionally deuterated large proteins based on the combination of the 3D TROSY-HNCA (Salzmann et al., 1998; Eletsky et al., 2001) and 3D TROSY-HNCO experiments (Salzmann et al., 1999b, c) with the 3D MQ-HACACO experiment of Figure 1. (a) A sequential walk through 2D $^{13}C^{\alpha}$-$^{1}H^{N}$, $^{13}C'$-$^{1}H^{N}$ and $^{13}C^{\alpha}$-$^{13}C'$ strips taken at the positions of the corresponding $^{15}N$ and $^{1}H^{\alpha}$ resonances in 3D TROSY-HNCA, 3D TROSY-HNCO and 3D MQ-HACACO spectra, respectively. (b) A fragment of the polypeptide backbone schematically showing the magnetization transfer pathways a, b and c achieved with TROSY-HNCO, TROSY-HNCA and MQ-HACACO, respectively.

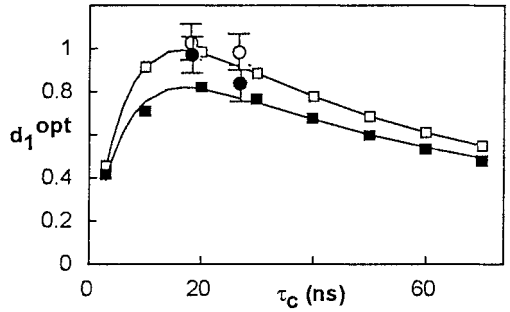


*Figure 5.* Optimal interscan delays, $d_1^{opt}$, calculated using the full relaxation matrix approach, displayed along with nonlinear fits to Equation 2 and the experientially observed values of $d_1^{opt}$ for the 44 kDa uniformly $^{15}N$,$^{13}C$-labeled and fractionally 35% deuterated BsCM (Eletsky et al., 2001) measured at 20 °C ($\tau_c$ = 20 ns) and at 9 °C ($\tau_c$ = 27 ns). Open and filled circles represent the mean value and the standard deviation of the experimentally determined $d_1^{opt}$ measured for the $^{1}H^{\alpha}$ spins resonating at 5.5±0.2 ppm in a series of 1D MQ-HACACO experiments run without and with $^{1}H^{N}$ band selective excitation pulses, respectively. The values shown correspond to the duration of the interscan delay which delivered the maximum value for the signal intensity divided by the square root of the total experimental measurement time. Squares represent calculated $d_1^{opt}$ using the numerical intergration of the system of linear differential equations describing longitudinal relaxation of the $^{1}H^{N}$, $^{1}H^{C}$, $^{13}C$ and $^{15}N$ spins. The open squares correspond to the following conditions: $I^{HN}(0) = I^{HC}(0) = I^{C}(0) = I^{N}(0) = 0$ whereas for the filled squares $I^{HN}(0) = 0.7\ I_{eq}^{HN}$, $I^{HC}(0) = I^{C}(0) = I^{N}(0) = 0$. The value $I^{HN}(0) = 0.7\ I_{eq}^{HN}$ corresponds to the steady state $^{1}H^{N}$ magnetization achieved using the $^{1}H^{N}$ flip-back trick. The model-free spectral density functions (Lipari and Szabo, 1982) with $S^2 = 0.9$, $\tau_e = 0.9$ ps and the standard interatomic distances (Koradi et al., 1996) were used.

bust procedure can be effectively applied to large 3D data sets with low signal-to-noise ratios.

The combined use of the 3D TROSY-HNCA, 3D TROSY-HNCO and 3D MQ-HACACO experiments for the residue specific assignment of the $^{1}H^{\alpha}$, $^{1}H^{N}$, $^{15}N$, $^{13}C^{\alpha}$ and $^{13}C'$ backbone resonances is outlined in Figures 4a and 4b. Sequential connectivities derived from weak sequential cross peaks in the 3D TROSY-HNCA experiments are complemented or completely replaced by strong one-bond $^{13}C^{\alpha}$-$^{13}C'$ correlation cross-peaks obtained from the MQ-HACACO experiment (Figure 4a). In addition, the use of the MQ-HACACO experiment provides a means to overcome the problem of the spectral overlap of the inter- and intraresidual $^{13}C^{\alpha}$ resonances in TROSY-HNCA (Salzmann et al., 1999b) by using the chemical shifts of the $^{1}H^{\alpha}$ spins to resolve overlapping $^{13}C^{\alpha}$ resonances (Figure 4b). For the BsCM protein only reasonable number of possible variants of the resonance assignment arising at the branching points with multiple $^{13}C^{\alpha}$ or $^{13}C'$ overlaps had to be checked. To further reduce the number of combinatorial variants of matching strips, the 4D TROSY-HACANH experiment (K. Hu and K. Pervushin, in preparation) can be used. For proteins with large correlation times but a relatively small number of residues such as membrane proteins embedded in micelles or oligomeric proteins this strategy alleviates the need to acquire the low sensitivity $^{13}C^{\alpha}$-constant-time TROSY-HNCA experiment (Salz-

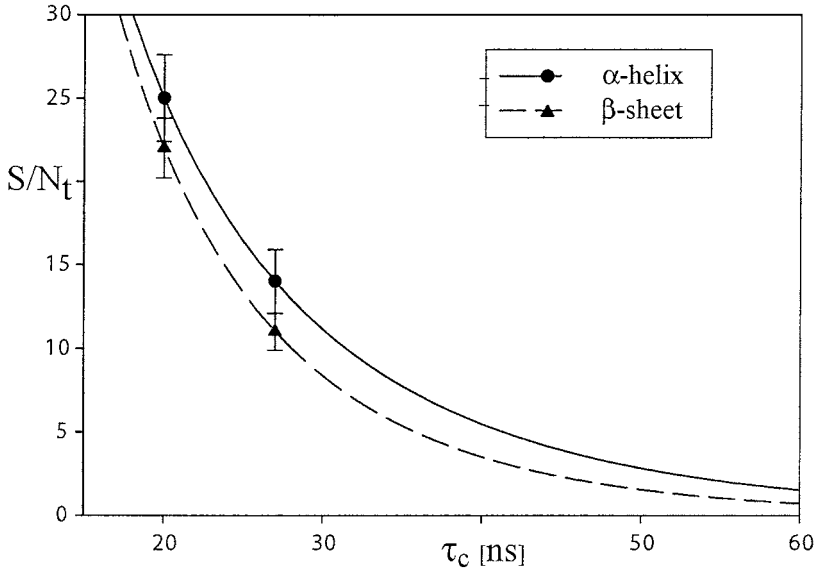


*Figure 6.* The experimentally achieved and predicted $S/N_t$ in the 3D MQ-HACACO spectra measured using the experimental scheme of Figure 1 for the cross-peaks stemming from the α-helical or β-sheet residues in the 44 kDa uniformly $^{15}N$,$^{13}C$-labeled and fractionally 35% deuterated BsCM (Eletsky et al., 2001) at 20 °C ($\tau_c$ = 20 ns) and 9 °C ($\tau_c$ = 27 ns). The optimized interscan delays $d_1^{opt}$ were set to 1.25 s and 1.12 s at 20 °C and 9 °C, respectively. $S/N_t$ was calculated as the average amplitude of the corresponding cross-peaks divided by the square root of the total experimental measurement time. The solid and dashed curves are calculated according to Equation 3 with the parameters $A$ = 215 and 261, and $B = 0.051 \times 10^9$ s$^{-1}$ and $0.067 \times 10^9$ s$^{-1}$ for the α-helical and β-sheet residues, respectively.

mann et al., 1999a) or a series of time-consuming 4D TROSY-type triple-resonance experiments (Konrat et al., 1999).

The applicability of the MQ-HACACO experiment to proteins with higher molecular weight can be estimated by considering the maximal signal-to-noise ratio per unit measurement time as a function of the rotational correlation time $\tau_c$ given by Equation 1. It is assumed that no apodization function is applied before Fourier transformation.

$$S/N_t^{max} \sim p\left(-\sum_i R_2^i \tau_i\right) / \left(\sqrt{d_1^{opt} + d_0} \cdot R^i\right). \quad (1)$$

$d_1^{opt}$ is the optimal interscan delay which depends on the longitudinal relaxation rates of the $^1H^\alpha$ spins (Ernst et al., 1987; Cavanagh et al., 1996), $d_0$ is the acquisition time, $R_2^{C'}$ is the transverse relaxation rate of the $^{13}C'$ spins and $R_2^i$ is the transverse relaxation rate of the $i$-th coherence evolving during the constant-time periods $\tau_i$ between time points $a$ and $d$ in Figure 1. In the adiabatic approximation all non-vanishing $R_2^i$ are proportional to the rotational correlation time $\tau_{c'} = \sum_i R_2^i \tau_i = B\tau_c$ (Ernst et al., 1987). Due to the multi-exponential recovery of the $^1H$ magnetization no closed form solution for $d_1^{opt}$ as a function of $\tau_c$ exists. Nevertheless, $d_1^{opt}(\tau_c)$ can be approximated by a non-linear fit of the empirical Equation 2 to the numerically computed $d_1^{opt}$ delays for a range of $\tau_c$ values using the full relaxation matrix approach.

$$d_1^{opt}(\tau_c) = a/(\tau_c + b + c/\tau_c). \quad (2)$$

The sum in Equation 2 represents raising and lowering 'wings' of a typical $T_1$ functional dependence on the rotational correlation time $\tau_c$ (Wüthrich, 1986). Figure 5 shows the numerically calculated $d_1^{opt}$ delays for a range of $\tau_c$ values. The best fit of Equation 2 is achieved with $a = 50.1 \times 10^{-9}$ s$^2$, $b = 17.6 \times 10^{-9}$ s and $c = 269 \times 10^{-9}$ s$^2$ (the lower curve in Figure 5). The experimentally determined $d_1^{opt}$ are sufficiently well reproduced (Figure 5, open and filled circles). The sensitivity of the MQ-HACACO can be enhanced by preventing the saturation of the $^1H^N$ spins before data acquisition which results in faster recovery of the $^1H^\alpha$ spins during the interscan delay due to the $^1H^N/^1H^\alpha$ dipole-dipole interactions as it is described in detail elsewhere (Pervushin et al., 2002). As seen from Figure 5, implementation of the $^1H^N$ flip-back decreases $d_1^{opt}$ by 20% with a concomitant 10% increase in spectral sensitivity.

Inserting the values for $a$, $b$ and $c$ into Equation 2 and substituting for $d_1^{opt}$ in Equation 1 results

in Equation 3.

$$S/N_t^{max} = A\sqrt{\tau_c + 17.6 \times 10^{-9} + 269 \times 10^{-9}/\tau_c} \exp(-B \cdot \tau_c)/\tau_c, \quad (3)$$

where we use the adiabatic approximation for both $R_2^i$ and $R_2^{C'}$. Equation 3 represents the maximal sensitivity of the MQ-HACACO experiment as a function of $\tau_c$.

The parameters $A$ and $B$ in Equation 3 can be determined by repeating the MQ-HACACO experiment with the same protein at two temperatures. Figure 6 shows the curves obtained for Equation 3 with the parametrization obtained for residues in the α-helical and β-sheet secondary structure elements of BsCM. As expected on the basis of the proton density in α-helices and β-sheets (Salzmann et al., 1999b) a slightly better $S/N_t$ was measured for the residues in α-helical regions as compared to β-sheet regions. Overall, we predict that the MQ-HACACO experiment can deliver sufficient sensitivity to support sequential assignment for proteins with rotational correlation time up to 40–50 ns, which at ambient temperatures corresponds to molecular weights in the range of 80–100 kDa. The absolute limit on the applicability of the proposed experiment is imposed by the collapse of the $^{13}C'$ antiphase multiplet due to fast transverse relaxation. For rigid proteins at 600 MHz polarizing magnetic field strength this may occur for $\tau_c \approx 90$ ns assuming that transverse relaxation of the $^{13}C'$ spins is solely determined by the CSA interaction with $\Delta\sigma(^{13}C') = 150$ ppm (Veeman, 1984). At this correlation time each of the $^{13}C'$ multiplet component will exhibit $\Delta\nu_{1/2}$ equal to $^1J_{C\alpha C'} = 53$ Hz resulting in cancellation of about 20% of the antiphase multiplet.

Thus, we propose the use of the 3D MQ-HACACO experiment as a complementary tool to the TROSY line of experiments for assignment of the backbone resonances in large proteins. The transverse relaxation optimization in the new experiment is achieved by employing a multiple-quantum evolution period to record $^1H^\alpha$ and $^{13}C^\alpha$ chemical shifts and to simultaneously transfer magnetization to the $^{13}C'$ spins for signal acquisition. A single correlation cross-peak per amino acid can be obtained by the post-acquisition processing of the spectra, improving sensitivity and greatly facilitating the analysis of spectra. We propose to use the most sensitive pair of TROSY triple resonance experiments, namely TROSY-HNCA and TROSY-HNCO, together with the 3D MQ-HACACO to obtain sequence-specific backbone resonance assignment in proteins with the molecular weight up to 80 kDa.

## References


Cavanagh, J., Fairbrother, W.J., Palmer, A.G. and Skelton, N.J. (1996) *Protein NMR Spectroscopy: Principles and Practice*. Academic Press, New York, NY.

Dayie, K.T. and Wagner, G. (1997) *J. Am. Chem. Soc.,* **119**, 7797–7806.

Eletsky, A., Kienhöfer, A. and Pervushin, K. (2001) *J. Biomol. NMR*, **20**, 177–180.

Ernst, R.R., Bodenhausen, G. and Wokaun, A. (1987) *The Principles of Nuclear Magnetic Resonance in One and Two Dimensions*. Clarendon Press, Oxford.

Geen, H. and Freeman, R. (1991) *J. Magn. Reson.,* **93**, 93–141.

Grzesiek, S., Kuboniwa, H., Hinck, A.P. and Bax, A. (1995) *J. Am. Chem. Soc.,* **117**, 5312–5315.

Koehl, P. (1999) *Prog. Nucl. Mag. Reson. Spectrosc.*, **34**, 257–299.

Konrat, R., Yang, D.W. and Kay, L.E. (1999) *J. Biomol. NMR,* **15**, 309–313.

Koradi, R., Billeter, M. and Wüthrich, K. (1996) *J. Mol. Graph.*, **14**, 51–55.

Lipari, G. and Szabo, A. (1982) *J. Am. Chem. Soc.*, **104**, 4546–4559.

Marion, D., Ikura, M., Tschudin, R. and Bax, A. (1989) *J. Magn. Reson.*, **85**, 393–399.

Mulder, F.A.A., Ayed, A., Yang, D.W., Arrowsmith, C.H. and Kay, L.E. (2000) *J. Biomol. NMR*, **18**, 173–176.

Pervushin, K.V. (2000) *Quart. Rev. Biophys.*, **33**, 161–197.

Pervushin, K., Riek, R., Wider, G. and Wüthrich, K. (1997) *Proc. Natl. Acad. Sci. USA*, **94**, 12366–12371.

Pervushin, K., Vögeli, B. and Eletsky, A. (2002) *J. Am. Chem. Soc.*, **124**, 12898–12902.

Salzmann, M., Pervushin, K., Wider, G., Senn, H. and Wüthrich, K. (1998) *Proc. Natl. Acad. Sci. USA*, **95**, 13585–13590.

Salzmann, M., Pervushin, K., Wider, G., Senn, H. and Wüthrich, K. (1999a) *J. Biomol. NMR*, **14**, 85–88.

Salzmann, M., Wider, G., Pervushin, K., Senn, H. and Wüthrich, K. (1999b) *J. Am. Chem. Soc.*, **121**, 844–848.

Salzmann, M., Wider, G., Pervushin, K. and Wüthrich, K. (1999c) *J. Biomol. NMR*, **15**, 181–184.

Salzmann, M., Pervushin, K., Wider, G., Senn, H. and Wüthrich, K. (2000) *J. Am. Chem. Soc.*, **122**, 7543–7548.

Serber, Z., Richter, C. and Dotsch, V. (2001) *Chembiochem,* **2**, 247–251.

Serber, Z., Richter, C., Moskau, D., Bohlen, J.M., Gerfin, T., Marek, D., Haberli, M., Baselgia, L., Laukien, F., Stern, A.S., Hoch, J.C. and Dotsch, V. (2000) *J. Am. Chem. Soc.,* **122**, 3554–3555.

Shaka, A.J., Keeler, J., Frenkiel, T. and Freeman, R. (1983) *J. Magn. Reson.,* **52**, 335–338.

Swapna, G.V.T., Rios, C.B., Shang, Z.G. and Montelione, G.T. (1997) *J. Biomol. NMR,* **9**, 105–111.

Veeman, W.S. (1984) *Prog. NMR Spectrosc.,* **16**, 193–235.

Wüthrich, K. (1986) *NMR of Proteins and Nucleic Acids*, Wiley, New York, NY.

Xia, Y.L., Kong, X.M., Smith, D.K., Liu, Y., Man, D. and Zhu, G. (2000) *J. Magn. Reson.,* **143**, 407–410.

Yang, D.W. and Kay, L.E. (1999) *J. Am. Chem. Soc.,* **121**, 2571–2575.